Eur Biophys J (2010) 39:781–787
DOI 10.1007/s00249-009-0550-x

ORIGINAL PAPER

Netropsin binding in five duplex-dimer DNA constructs as a function of size and distance between binding sites: circular dichroism and absorption spectroscopy

Lavanya Premvardhan · Jean-Claude Maurizot

Received: 7 May 2009 / Revised: 10 September 2009 / Accepted: 24 September 2009 / Published online: 28 October 2009
© European Biophysical Societies' Association 2009

Abstract The optical activity induced on binding the drug netrospin (NET) in the minor groove of DNA is studied in five oligonucleotides (OGNs) as a function of (1) the size of the binding site in $(5'\text{-}(GC)_2AATT(GC)_2\text{-}3')_2$ (OGN 1a) versus $(5'\text{-}(GC)_2AAATTT(GC)_2\text{-}3')_2$ (OGN 1b) and (2) the distance between two AATT binding sites in $(5'\text{-}(GC)_2AATT(GC)_xAATT(GC)_2\text{-}3')_2$, with $x = 1$, 2, or 3 (OGNs 2a, b, c, respectively). NET binding is monitored via the induced circular dichroism (CD) at ~315 nm, where the nucleic acids are optically inactive. The CD titrations, fit to a tight binding model, yield lower limits for the binding constant, K_a, $\geq 8 \times 10^7\ M^{-1}$ for OGN 1a and $\geq 2 \times 10^8\ M^{-1}$ for OGNs 2a, b, c in 1 mM buffer. In 100 mM buffer, tight binding occurs in all five OGNs with $K_a \geq 8 \times 10^7\ M^{-1}$ for OGN 1a and $\geq 1 \times 10^8\ M^{-1}$ for OGNs 1b and 2a, b, c. In contrast, the elongated AAATTT binding site of OGN 1b results in weak binding of NET in 1 mM buffer, where competing electrostatic interactions with the solvent environment are lower. In the constructs with two binding sites, the increase in flexibility introduced by intervening GC base pairs does not induce co-operative binding, although differences in the number of binding sites, *n* (2.05–2.65), indicate that there may be differences in the way NET is bound in OGNs 2a, b, c. In addition, the large shifts in the absorption spectra induced in bound versus free NET, and effects on the CD spectral bands at higher energy, are discussed in terms of electrostatic and excitonic interactions.

Keywords Drug-DNA binding · Circular dichroism · Excitonic · Electrostatic interactions · Netropsin

Abbreviations

CD	Circular dichroism
NET	Netropsin
OGN	Oligonucleotide
OGN 1a	$(5'\text{-}(GC)_2AATT(GC)_2\text{-}3')_2$
OGN 1b	$(5'\text{-}(GC)_2AAATTT(GC)_2\text{-}3')_2$
OGN 2a	$(5'\text{-}(GC)_2AATT(GC)AATT(GC)_2\text{-}3')_2$
OGN 2b	$(5'\text{-}(GC)_2AATT(GCGC)AATT(GC)_2\text{-}3')_2$
OGN 2c	$(5'\text{-}(GC)_2AATT(GCGCGC)AATT(GC)_2\text{-}3')_2$

Introduction

Netropsin (NET) is a drug that is known to bind into the minor groove (AT site) of DNA (Berman et al. 1979; Patel and Canuel 1977; Zimmer et al. 1972), and although its anti-viral and anti-bacterial properties cannot be exploited clinically, NET has served as a model compound to study the structural effects of drug-DNA interactions (Nunn et al. 1997; Patel and Canuel 1977; Sriram et al. 1992; Tabernero et al. 1993; van Hecke et al. 2005; Vlieghe et al. 1999). Binding of NET to an oligonucleotide (OGN) is primarily characterized by the electrostatic interactions between its positively charged end groups with the nitrogen of adenine, and the oxygen of thymine, at the "floor of the minor groove," as well as van der Waal's interactions with the sugar-phosphate backbone at the sides of the groove

L. Premvardhan · J.-C. Maurizot
Centre de Biophysique Moléculaire, UPR4301 CNRS,
45071 Orléans Cedex 2, France

L. Premvardhan (✉)
Synchrotron SOLEIL, Saint-Aubin,
91192 Gif-sur-Yvette Cedex, France
e-mail: lavanya.premvardhan@synchrotron-soleil.fr;
premvard@gmail.com

(van Hecke et al. 2005). The conformation adopted by NET when bound to DNA is broadly distinguished into: class I, where NET displaces the spine of hydration and is centrally bound in the minor groove (Nunn et al. 1997; Tabernero et al. 1993; van Hecke et al. 2005), and class II, where NET shifts half a base pair to adopt a side-by-side binding with a guanine (Sriram et al. 1992). Detailed structural characterization also shows that water molecules can mediate the binding of NET, which then forces it into a more linear conformation (Freyer et al. 2007).

The known specificity of NET to the AT site, and the availability of precisely synthesized OGNs, can be exploited to study the relationship between NET structure and the electrostatic and thermodynamic properties of its binding (Freyer et al. 2007; Gondeau et al. 1998; Marky and Breslauer 1987; Patel and Canuel 1977). Here, five different OGNs have been selected, where (1) the "size" of the binding site differs between OGN 1a (AATT) and OGN 1b (AAATTT) and (2) the distance between the two AATT binding sites differs by one, two, or three interposed GC residues in OGN 2a, OGN 2b, and OGN 2c, respectively (Table 1). The crystal structures of various NET-DNA (construct) complexes, including that with an elongated AAATTT binding site (Tabernero et al. 1993), generally show a fairly straightforward binding of a single NET molecule into the central part of the minor groove. Drug binding in solution, however, results from ensemble averaged dynamics, and thermodynamic conditions are quite different from those in the solid-phase crystal structure. Solution-phase studies of NET binding that best mimic biological conditions could thus offer additional information about in vivo conditions and are, moreover, important for improving the robustness and accuracy of calculations (Dolenc et al. 2005; van Hecke et al. 2005; Vlieghe et al. 1999).

The current study exploits the optical activity induced in NET on binding into the minor groove of DNA: the propeller twist conformation adopted on binding induces chirality in what is otherwise a nonchiral molecule (Zimmer and Luck 1970), and the new CD band that appears at 300–325 nm provides a quantitative measure for binding. NET, a free and "floppy" oligopeptide in solution, is constrained to a conformation that fits to the helical form of the duplex OGN. For example, the dihedral angle between the two pyrrole rings of NET is $\sim 20°$ for the free drug (Berman et al. 1979), whereas it is estimated to be $\sim 40°$ when bound in the AATT duplex (van Hecke et al. 2005). Here, NET binding is studied in both high- and low-ionic strength buffer solutions with the latter environment presumed to provide more accurate values for the binding affinities of NET. The binding (association) constant, K_a, and number of binding sites, n, are determined by fitting the CD titration curves to a tight-binding model (Greenfield 2006; Lah and Vesnaver 2004; Martin and Schilstra 2007; Rodger et al. 2005).

In addition to optical activity, absorption changes are also induced in NET on binding into the minor groove because of the changes in structure and the electrostatic interactions with adjacent base pairs and, possibly, the second NET molecule. Here, the absorption shifts of NET in the five OGNs are characterized by comparison with the absorptions of the netropsin-oligo (NET-OGN) complexes relative to that of intrinsic NET and the OGN absorptions (λ_{max} NET = 296 nm and λ_{max} OGNs = 260 nm). Also discussed is the effect of the perturbation of the electronic properties of the higher excited states of NET and the OGNs, as well as the effect on the lower energy transition of NET, with a view to future synchrotron CD (SRCD) studies clarifying these propositions.

Materials and methods

Sample preparation

NET (Sigma Aldrich) and OGNs 1b, 2a, 2b, and 2c (Amersham Pharma, AP) were used without further purification. About 1–2 mL of mM NET solutions in phosphate buffer (100 or 1 mM) were prepared fresh prior to each experiment and titrated in 5- to 10-μL aliquots. OGN

Table 1 Physical parameters of model DNA duplex dimer constructs

	Sequence	n-mer	T_m (°C)	ε (25°C)	ε (85°C)
OGN 1a	(5′-(GC)$_2$**AATT**(GC)$_2$-3′)$_2$	12-mer	70	182,800	205,280
OGN 1b	(5′-(GC)$_2$**AAATTT**(GC)$_2$-3′)$_2$	14-mer	65	206,800	231,416
OGN 2a	(5′-(GC)$_2$**AATT**(GC)**AATT**(GC)$_2$-3′)$_2$	18-mer	63	264,800	317,387
OGN 2b	(5′-(GC)$_2$**AATT**(GC)$_2$**AATT**(GC)$_2$-3′)$_2$	20-mer	67	298,000	362,310
OGN 2c	(5′-(GC)$_2$**AATT**(GC)$_3$**AATT**(GC)$_2$-3′)$_2$	22-mer	70	332,000	396,160

The abbreviations of the OGNs are listed along with the duplex dimer sequences, with the binding sites for NET shown in bold. The physical parameters for these constructs listed include their lengths (n-mer), the melting temperatures (T_m) in degree Celsius determined from CD spectra, and the extinction coefficients (ε) calculated from the 25°C absorption spectra and extrapolated to the 85° absorbances

solutions of μM (0.7–3.0) concentration in phosphate buffer were freshly prepared from concentrated stock maintained at −5°C in deionized water. The concentration of NET was determined using the extinction coefficient (ε) of 215,000 $M^{-1}cm^{-1}$. The OGN concentrations were obtained from the nearest-neighbor εs of the single-strand DNA base pairs extrapolated to the absorbances of the denatured OGNs measured at 85°. The uncorrected εs, from the absorbances at 25°C, are 10–20% smaller (Table 1). The results reported here for OGN 1a are from Eurogenetic (EG), as the sample from AP gave inconsistent results. OGN 2b, double of OGN 1a, from EG was verified to give similar results to that from AP.

Instrumentation

CD spectra at 25°C and melting curves were obtained on a (Peltier controlled) JASCO (J810) spectrometer. Denatured OGN absorption spectra at 85°C were obtained using a circulating ethylene glycol bath in a Uvikon SFM-25 spectrometer. 1-cm pathlength cuvettes (2.5 mL) were used in all cases.

Methodology

The melting temperatures, T_m, of the OGNs were obtained in 1 mM phosphate buffer solutions from 5 to 85°C at a heating rate of 30°C/h. Melting curves of the OGNs were shown to be monophasic and reversible with T_m values between 65 and 70°C (Table 1). The drug-binding reaction was followed by the addition of 10–15 aliquots of 5–10 μL of NET solution (∼1 μM) to 2.5 mL of OGN solutions (OD = 0.3–0.8). The binding ratios were obtained from at least three independent CD experiments (Table 2), with each spectrum being the average of three to five scans. CD and absorption measurements performed in 100 mM buffer were obtained from a single set of experiments, each the average of five scans.

The CD data are converted from ellipticity (θ) to the (molar) change in circular dichroic extinction coefficient, $\Delta\varepsilon$, using the relationship $\Delta\varepsilon = \theta/(32{,}980\ cl)$, where c is the molarity of the OGN and l the pathlength in centimeters. The changes in CD intensity, normalized to the concentration of the OGNs, are fit according to a tight-binding model as given by Greenfield (Greenfield 1999, 2006):

$$[\theta]_i = [\theta]_{\max}\left\{\left(\frac{1}{2K_a[P_t]} + \frac{[A_0]_i}{2n[P_t]} + \frac{1}{2}\right) - \left(\left(\frac{1}{2K_a[P_t]} + \frac{[A_0]_i}{2n[P_t]} + \frac{1}{2}\right)^2 - \frac{[A_0]_i}{n[P_t]}\right)^{0.5}\right\}. \quad (1)$$

Here $[A_0]_i/[P_t]$ is the $[NET]_i/[OGN]$ ratio (x in Fig. 2). The best fit to $[\theta]_i$ versus x yields n, the number of binding sites, and K_a, the association/binding constant. The CD titration of OGN 1b in 1 mM buffer is fit to the built-in Hill function in OriginLab, appropriate for weak binding (Greenfield 2006).

The conditions under which the reactants and products co-exist at notable concentrations should yield the most reliable value for the binding constants, and the titrations smoothly curve to a maximum θ_i value with no sharp transition at full occupation (Martin and Schilstra 2007), however, this was not typically the case in the titrations here. [Starting OGN concentrations are higher than the optimum values suggested at 5–10 × K_a (Martin and Schilstra 2007), although other evaluations suggest that for $k_n \sim 10^8\ M^{-1}$, [OGN] should be $\leq 10^{-6}$ M (Lah and Vesnaver 2004)]. Therefore, the binding constants from the fits are a lower bound. In 1 mM buffer, the reported K_a for each OGN (Table 2) is the largest of the lower bound values obtained independently from three measurements, with the K_a value constrained to result in errors that are

Table 2 NET binding constants and binding ratios in DNA duplex dimer constructs

OGN	1 mM Buffer		100 mM Buffer	
	K_a (M^{-1}) ([OGN])	n	K_a (M^{-1}) ([OGN])	n
OGN 1a	8×10^7 (3.2×10^{-6})	1.10 ± 0.16	8×10^7 (2.82×10^{-6})	1.00 ± 0.03
OGN 1b	– ($1–3 \times 10^{-6}$)	–	1×10^8 (2.74×10^{-6})	1.14 ± 0.01
OGN 2a	4×10^8 (0.9×10^{-6})	2.33 ± 0.23	9×10^7 (2.62×10^{-6})	2.27 ± 0.06
OGN 2b	2×10^8 (0.8×10^{-6})	2.22 ± 0.33	1×10^8 (1.92×10^{-6})	2.51 ± 0.07
OGN 2c	3×10^8 (1.5×10^{-6})	2.46 ± 0.16	1×10^8 (1.39×10^{-6})	2.80 ± 0.04

The best fit to the binding of NET in OGN 1a, b and 2a–2c using a tight binding model (see Fig. 2) yielded values for the binding constants and the binding ratios in 1 and 100 mM phosphate buffer. The K_a values reported in 1 mM buffer are the largest of the lower bounds obtained independently from three different measurements. The corresponding OGN concentrations [OGN], from ε values extrapolated from 85°C absorptions (Table 1), are reported *in parentheses*. The errors in n in 1 mM buffer are obtained from the error from three independent measurements, typically larger than from a single fit as reported in 100 mM

50% smaller than the estimated parameter (no such constraint was placed on n). If the parameters are manually chosen to give the best lower-bound fit (shown in Fig. 2), then somewhat higher K_a values are obtained at $\sim 10^8$ M^{-1} for OGNs 1a, b, and 5–10 $\times$ 10^8 M^{-1} for OGNs 2a, b, c. Note that the K_a values for OGNs 2a, b, c, are the products of the equilibrium constants, k_n, for binding at each of the two sites. The sharp transition of the titrations that allows only a lower bound value of K_a, conversely permits a more accurate determination of the number of binding sites (n).

Results and discussion

Binding constants and stoichiometry from CD spectra

The absorption spectra of NET, along with those of the five OGNs, are shown in Fig. 1 at 25°C. The absorption spectra of the OGNs are quite similar to each other, and the low-energy band at 260 nm is flanked by the two electronic transitions of NET (Fig. 1b: $\lambda_{max} = 238$ and 296 nm in 1 mM buffer). The induced optical activity of the NET-OGN complexes monitored at $\sim$315 nm corresponds to the lower-energy absorption band of NET (rectangles in Fig. 1, and Fig. 3).

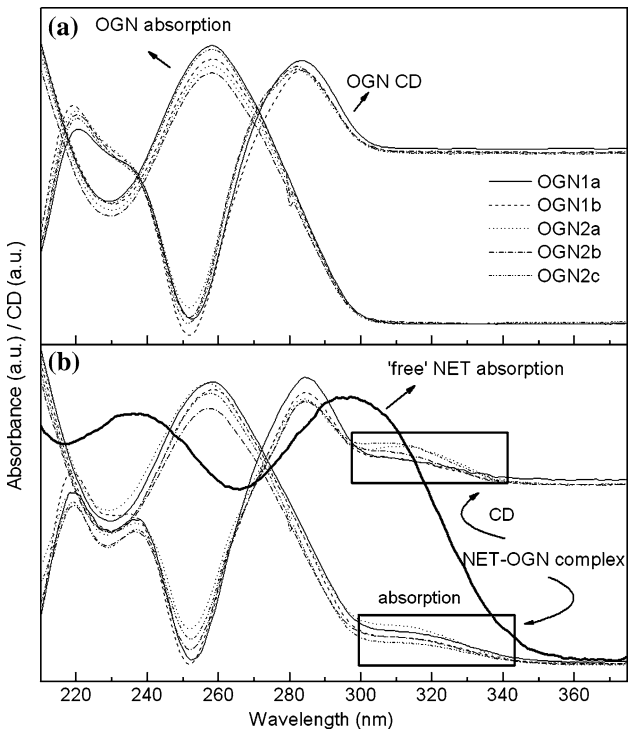

Fig. 1 **a** Absorption and CD spectra of OGN 1a–OGN 2c, **b** CD spectra of NET-OGN complexes and the absorption of NET (*solid line*), in 1 mM phosphate buffer solutions. The absorption and CD spectra have been arbitrarily scaled to have similar intensities. Optical densities of the OGNs range from 0.3 to 0.7, and $\Delta\varepsilon$(CD) are $\sim$60 at 315 nm (Fig. 2)

The induced CDs in all cases increase linearly, up to close to the saturation of (both) the binding sites in the OGNs, demonstrating a straightforward noncooperative 1:1 (or 2:1) binding of NET:OGN, except in the case of OGN 1b in 1 mM buffer. The K_a values reported in Table 2, in 1 mM buffer, are the largest minimum values from the best fit to the three independent titrations: OGN 1a has a $K_a \geq 8 \times 10^7$ M^{-1}, whereas the (apparent) K_a of OGNs 2a, b, c are $\geq 2 \times 10^8$ M^{-1}. In high ionic strength media, a similar lower bound is found for OGN 1a, and slightly smaller K_as of 1×10^8 M^{-1} for OGNs 2a, b, c. [Manually inputting the K_a and n values to obtain the lower bound of the best fit ($r^2 > 0.98$) yields nearly the same n values, but K_as that are 5–10 times larger.] The values determined for OGNs 1a, b are similar to the binding constants of NET to single AATT sites in hairpin constructs, determined from isothermal calorimetry measurements to be on the order of 10^7–10^8 M^{-1} (Freyer et al. 2007).

The apparent K_as for OGN 2s, with two AATT sites, are somewhat larger than for OGNs 1a, b but should actually be orders of magnitude larger, as the binding affinity of NET to the second AATT site should be similar to the first one. Note, however, that the binding of the first NET could affect the binding environment of the second NET. For example, the expansion of the minor groove (Nunn et al. 1997), or displacing water molecules from the spine of hydration of the double helix (Freyer et al. 2007), could influence the conformation of the second AATT site and reduce the favorability of binding the second NET. If NET adopts a more linear conformation (Freyer et al. 2007), the magnitude of the CD band could be diminished (Lah and Vesnaver 2004), or conversely if NET has a more pronounced propeller twist, the CD signal could be enhanced. However, such effects seem to be minimal here, and the geometry of the second NET does not appear to be significantly affected, else it would be expected to affect the transition dipole moments, and concomitantly the rotational strengths, and thus change the slope of the CD titration curve after the first NET is bound. Thus, both NET molecules bound to OGN2s must adopt the same, or very similar, conformation, else a break in the titration curve would be apparent after the first NET is bound. This is not the case here, and overall, NET binding follows a straightforward noncooperative, sequential binding process in OGN2s.

The other parameter determined from the fits is the number of binding sites, n (binding stoichiometry), which may also reflect mechanistic differences in the binding of NET. The binding stoichiometry of NET to OGN 1a is close to 1, whereas in OGNs 2a, b, c, values of somewhat >2 binding sites are estimated (Table 2), which could suggest the influence of the terminating, or intervening, base pairs on the pattern of NET binding. Certainly, an overestimation of OGN εs and the resultant

underestimation of concentrations, or the inverse in the case of NET concentration, could inflate the ratio of [NET]/[OGN] (x in Fig. 2). Relative differences in n are, however, noticeable, such as the larger n for OGN 2c, compared to OGNs 2a, b, and may be directly related to the distance between the two AATT sites, such that there is an increase in binding affinity with the larger separation. A trend in n with increasing number of intervening GC base pairs is more apparent in 100 mM buffer, from OGN 2a to 2b to 2c (Table 2), but will need to be investigated in greater detail using other methods.

Among the duplex constructs, OGN 1b noticeably deviates in its binding of NET in low-ionic strength buffer. There is a slight stabilization (plateau) at $r \sim 1$, but then the increase continues until it starts leveling off at [NET]/[OGN 1b] > 3. Crystal structures show one NET molecule extending over five of the six AT base pairs (Tabernero et al. 1993), which is the case in the high ionic-strength environment (100 mM buffer), where NET is strongly bound to OGN 1b with $n \sim 1.1$ and $K_a \geq 1 \times 10^8$. In 1 mM buffer, however, the environment appears to affect the conformation of the minor groove and thus the affinity of NET. For example, elongation of the AAATTT site could result in much weaker electrostatic interactions that permit more than one NET to be stacked onto the minor groove of OGN 1b at a given time. Elongation could indeed result from the weaker ionic forces of the surrounding environment and thus decrease the affinity to binding the drug. This result underscores the differences in the binding properties of NET in the condensed phase relative to the solid phase (Tabernero et al. 1993), and in the sensitivity and applicability of CD spectroscopy to pick out these differences as a function of the environment.

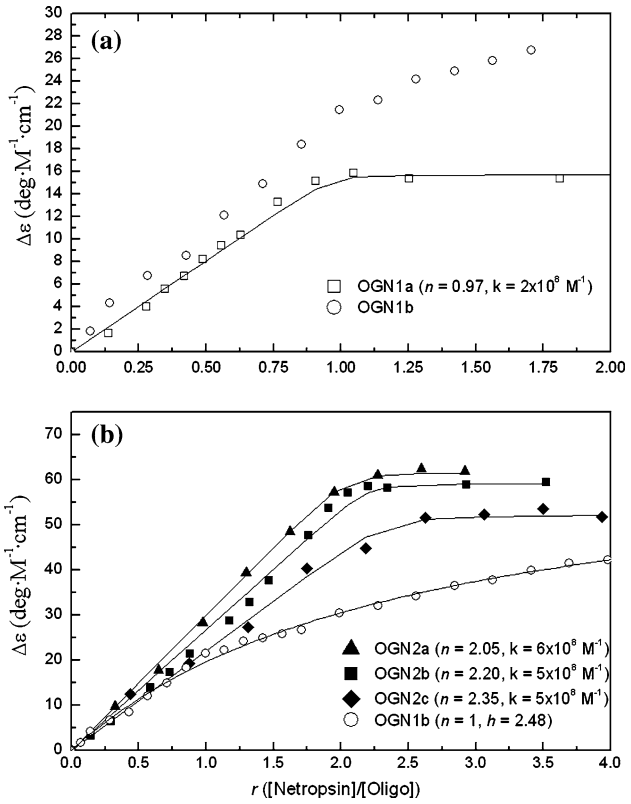

Fig. 2 CD titration values for NET-OGN complexes of $\Delta\varepsilon$ versus [NET]/[OGN] in 1 mM phosphate buffer are shown for **a** OGN 1a (*open square*) and **b** OGN 1b (*open circles*), OGN 2a (*solid triangle*), OGN 2b (*solid square*), and OGN 2c (*solid diamond*). The fits to these values using a tight-binding model (Eq. 1) are shown for titrations from the OGN concentrations listed in Table 2 with the binding stoichiometry (n) and (apparent) binding constants (K_a) from the fit listed in the legend

Absorption spectral differences of NET-OGN complexes

Additional information about the specific electrostatic interactions of NET and the OGNs is obtained from the absorption spectral changes of bound NET, where signification shifts in the electronic transition energies occur. In contrast, the absorption of the OGNs with bound NET is hardly affected (not shown) and the effects presumed to be minor. The absorption of the bound NET (Fig. 4), i.e., the difference in the NET-OGN complex absorption relative to the OGN absorption, indicates that the low-energy absorption band (1 mM buffer) undergoes two main changes on binding in all five cases: (1) a red shift of about 1,400 cm^{-1} (from 296 to ~309 nm), and (2) a narrowing of the absorption. These changes are interpreted as follows.

The increased affinity of NET for the AATT site, particularly in 1 mM buffer, indicates that the 'solvating' environment in the minor groove is more polar than in the buffer. A red shift in solute absorption is typical of increasing polarity and/or polarizability of the environment, provided the excited-state dipole moment of the solute is larger than in the ground state (Böttcher 1952; Premvardhan et al. 2005). This bathochromism could also be an indication of a loose J-type, or head-to-tail (Simonyi et al. 2003), aggregation of NET. Strong (excitonic) interactions between NET and the OGN base pairs, and/or the two NETs, should result in an enhanced magnitude of optical activity, such as the $\Delta\varepsilon$s of OGN2s being more than a factor of two greater than that of OGN1s (Fig. 3), although, e.g., the ε of OGN 2c is $\sim 2 \times \varepsilon$ of OGN 1a (Table 1). In addition, the red (bathochromic) shift of the CD maximum (Fig. 3) relative to the absorption (Fig. 1), particularly in the NET-OGN 2a complex, also suggests long-range excitonic interactions. However, these red shifts are evident in all five OGNs, which suggests that interactions with the base pairs having a stronger influence on the CD intensities than interaction between the two NETs.

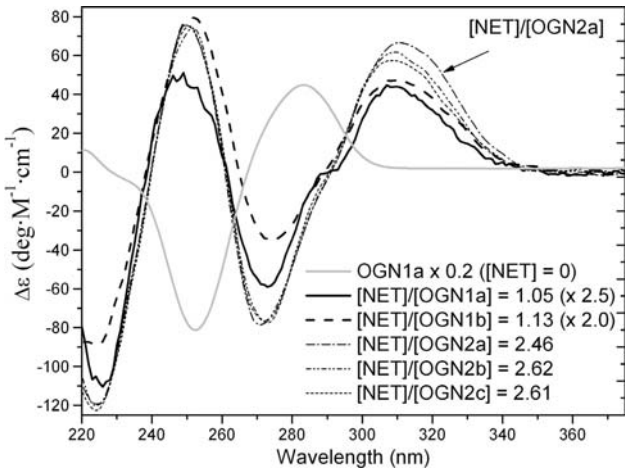

Fig. 3 CD spectra in 1 mM buffer of OGN 1a in the absence of NET (*solid gray*), and of bound NET, determined from the differences in the CD of NET-OGN complexes at [NET]/[OGN] values greater than *n* (Table 2), minus the CD spectrum of the corresponding OGN in the absence of NET. In the case of NET-OGN 1b, the CD spectrum is close to $r = 1$ (see Fig. 2a). The CD spectra of pure OGN 1a, NET-OGN 1a, and NET-OGN 1b have been scaled by 0.2, 2, and 2.5, respectively

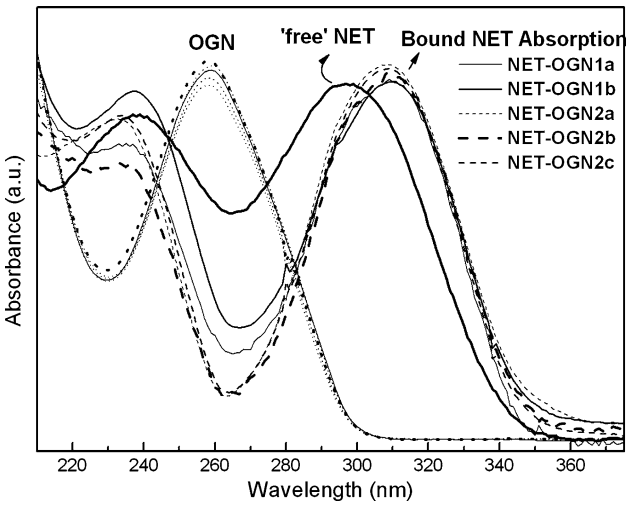

Fig. 4 The absorption spectra of pure OGN (λ_{max} ~260 nm), unbound NET (*dark solid line*), and bound NET (NET-OGN curves with λ_{max} ~310 nm) are shown. The five bound-NET spectra correspond to the difference in the NET-OGN absorptions, close to the mid-point of the binding ratios (Table 2), minus the corresponding OGN absorption spectrum. The intensities of the bound-NET (original OD < 0.1) have been scaled to the OGN absorption spectra

The characteristics of NET binding are also evident in the decrease in full-width half maxima of the absorption, reflecting the well-defined interactions of NET with the base pairs in the minor groove, in contrast to the broader range of interactions in the buffer solution. This decrease in inhomogeneous broadening of the absorption of the bound drug decreases overlap of the two electronic transitions of NET (Fig. 4) and actually provides suitable conditions to study the intrinsic electronic properties of these two states more easily. Note that the absorption spectra of bound NET have been magnified 10×, and the differences visible at higher energy (Fig. 4) partly arise from the error inherent in subtracting small changes in absorption. Nevertheless, the shifts in the absorption are evident and reflect that binding of the drug does result in strong effects on its electronic and electrostatic properties. These aspects of drug binding are well known, but techniques such as Stark spectroscopy could be exploited to better understand the extent and nature of the electronic perturbations (Chowdhury et al. 2001; Premvardhan et al. 2005).

CD spectrum of the NET-OGN complexes below 290 nm

Changes in the CD spectra of bound NET occur across the entire spectral range of the absorption spectrum (Fig. 1), and optical activity is also induced in the higher energy transition (λ_{max} ~237 nm in Fig. 4). The 'pure' CD spectrum of bound NET (Fig. 3), i.e., CD of the NET-OGN complex minus that of the corresponding OGN, has minima at 272 nm (36,800 cm^{-1}) and 224 nm (44,600 cm^{-1}) and maxima at 252 nm (40,000 cm^{-1}) and 315 nm (31,750 cm^{-1}). Note that the OGN CD spectrum, prior to the addition of NET, has been subtracted from the CD of the NET-OGN CD, and it is therefore unlikely that the CD band at (+)252 nm originates from the OGN, which has an intrinsic minimum close by at (−)254 nm (gray line in Fig. 3).

The lower energy CD band at 315 nm is red-shifted relative to the absorption maximum at 309 nm, whereas the higher energy transition of NET at 237 nm appears to have a nonconservative character, being split with a maximum at (+)224 nm and a minimum at (−)252 nm. These CD bands of bound-NET are *equally* separated by ~2,480 cm^{-1} from the maximum of the higher energy band of NET (~237 nm), indicating that this could correspond to the Davydov splitting arising from exciton interactions. Caution, however, needs to be used in interpreting the absorption shifts arising from J- or H-type aggregates (Simonyi et al. 2003), as the lower energy band of NET-OGN exhibits a red shift, whereas the higher energy band exhibits a small blue shift. The difference in the absorption and CD band characteristics of the higher and lower energy transitions of NET, however, suggest that there may be greater (excitonic) interaction of the 237-nm band of NET with the transitions of the OGN base pairs. Such would be the case if the transition dipole moments of the two NET transitions have different orientations, and if the transition dipole of higher energy band is oriented closer to 70° with respect to the transition dipoles of the base pairs.

The shoulder in the CD spectra at ~290 nm and possibly the (−)272 nm band, reflect the effects on the electronic properties of the OGN, i.e., on the adenines and thyamines, as a result of electrostatic interactions with the bound NET. The differences between the bound-NET CD in OGNs 1a, b versus 2a, b, c indicate differences in this region (Fig. 3) that suggest a more pronounced perturbation in the electronic properties of the base pairs in OGNs 1a, b. The sugar backbone could also play a specific role in these effects because its transition is closer to the higher energy band of NET. A more precise study in this wavelength range, and down to 160 nm, is envisioned with SR CD to better characterize the effects of drug binding on the DNA (constructs) and on the drug.

Acknowledgments L. Premvardhan acknowledges Région Centre (France) for financial support, and Dr. Frank Wien for useful suggestions.

References

Berman HM, Niedle S, Zimmer C, Thrum H (1979) Netropsin, a DNA-binding oligopeptide structural and binding studies. Biochim Biophys Acta 561:124–131

Böttcher CJF (1952) Theory of electric polarisation. Elsevier, Amsterdam

Chowdhury A, Wachsmann-Hogiu S, Bangal PR, Raheem I, Peteanu LA (2001) Characterization of chiral H- and J-aggregates of cyanine dyes formed by DNA templating using stark and fluorescence spectroscopies. J Phys Chem B 105:12196–12201

Dolenc J, Borstnik U, Hodoscek M, Koller J, Janezic D (2005) An ab initio QM/MM study of the conformational stability of complexes formed by netropsin and DNA. The importance of van der Waals interactions and hydrogen bonding. J Mol Struct 718:77–85

Freyer MW, Buscaglia R, Cashman D, Hyslop S, Wilson WD, Chaires JB, Lewis EA (2007) Binding of netropsin to several DNA constructs: evidence for at least two different 1:1 complexes formed from an -AATT-containing ds-DNA construct and a single minor groove binding ligand. Biophys Chem 126:186–196

Gondeau C, Maurizot J-C, Durand M (1998) Spectroscopic investigation of an intramolecular DNA triplex containing both G.G:C and T.A:T triads and its complex with netropsin. J Biomol Struct Dyn 15:1133–1144

Greenfield NJ (1999) Application of circular dichroism in protein and peptide analysis. Trends Analyt Chem 18:236–244

Greenfield NJ (2006) Determination of the folding of proteins as a function of denaturants, osmolytes or ligands using circular dichroism. Nat Protoc 1:2733–2741

Lah J, Vesnaver G (2004) Energetic diversity of DNA minor-groove recognition by small molecules displayed through some model ligand-DNA systems. J Mol Biol 342:73–89

Marky LA, Breslauer KJ (1987) Origins of netropsin binding affinity and specificity: correlations of thermodynamic and structural data. Proc Natl Acad Sci 84:4359–4363

Martin SR, Schilstra MJ (2007) Circular dichroism and its application to the study of biomolecules. Methods Cell Biol 84:263–293

Nunn C, Garman E, Neidle S (1997) Crystal structure of the DNA decamer d(CGCAATTGCG) complexed with the minor groove binding drug netropsin. Biochemistry 36:4792–4799

Patel DJ, Canuel LL (1977) Netropsin.poly(dA-dT) complex in solution: structure and dynamics of antibiotic-free base pair regions and those centered on bound netropsin. Proc Natl Acad Sci 74:5207–5211

Premvardhan L, Papagiannakis E, Hiller RG, van Grondelle R (2005) The charge-transfer character of the S0→S2 transition in the carotenoid peridinin is revealed by stark spectroscopy. J Phys Chem B 109:15589–15597

Rodger A, Marrington R, Roper D, Windsor S (2005) Circular dichroism spectroscopy for the study of protein-ligand interactions. In: Nienhaus GU (ed) Protein-ligand interactions: methods and applications, vol 305. Humana, Totowa, NJ, pp 343–364

Simonyi M, Bikadi Z, Zsila F, Deli J (2003) Supramolecular exciton chirality of carotenoid aggregates. Chirality 15:680–698

Sriram M, van der Marel GA, Roelen HLPF, van Boom JH, Wang AH-J (1992) Structural consequences of a carcinogenic alkylation lesion on DNA: effect of O6-ethylguanine on the molecular structure of the d(CGC[e6G]AATTCGCG)-netropsin complex. Biochemistry 31:11823–11834

Tabernero L, Verdaguer N, Coll M, Fita I, van der Marel GA, van Boom JH, Rich A, Aymami J (1993) Molecular structure of the A-tract DNA dodecamer d(CGCAAATTTGCG) complexed with the minor groove binding drug netropsin. Biochemistry 32:8403–8410

van Hecke K, Nam PC, Nguyen MT, van Meervelt L (2005) Netropsin interactions in the minor groove of d(GGCCAATTGC) studied by a combination of resolution enhancement and ab initio calculations. FEBS J 272:3531–3541

Vlieghe D, Sponer J, van Meervelt L (1999) Crystal structure of d(GGCCAATTGG) complexed with DAPI reveals novel binding mode. Biochemistry 38:16443–16451

Zimmer C, Luck G (1970) Optical rotatory dispersion properties of nucleic acid complexes with the oligopeptide antibiotics distamycin A and netropsin. FEBS Lett 10:339–342

Zimmer C, Luck G, Thrum H, Pitra C (1972) Binding of analogues of the antibiotics distamycin A and netropsin to native DNA. Eur J Biochem 26:81–89